SKIN LESION CLASSIFICATION USING MACHINE LEARNING

Anindya Shaha, Prem Prasad

The *Classical* Approach, Computer-Aided Diagnosis

Universitat de Girona

MAIA

COLOR CONSTANCY

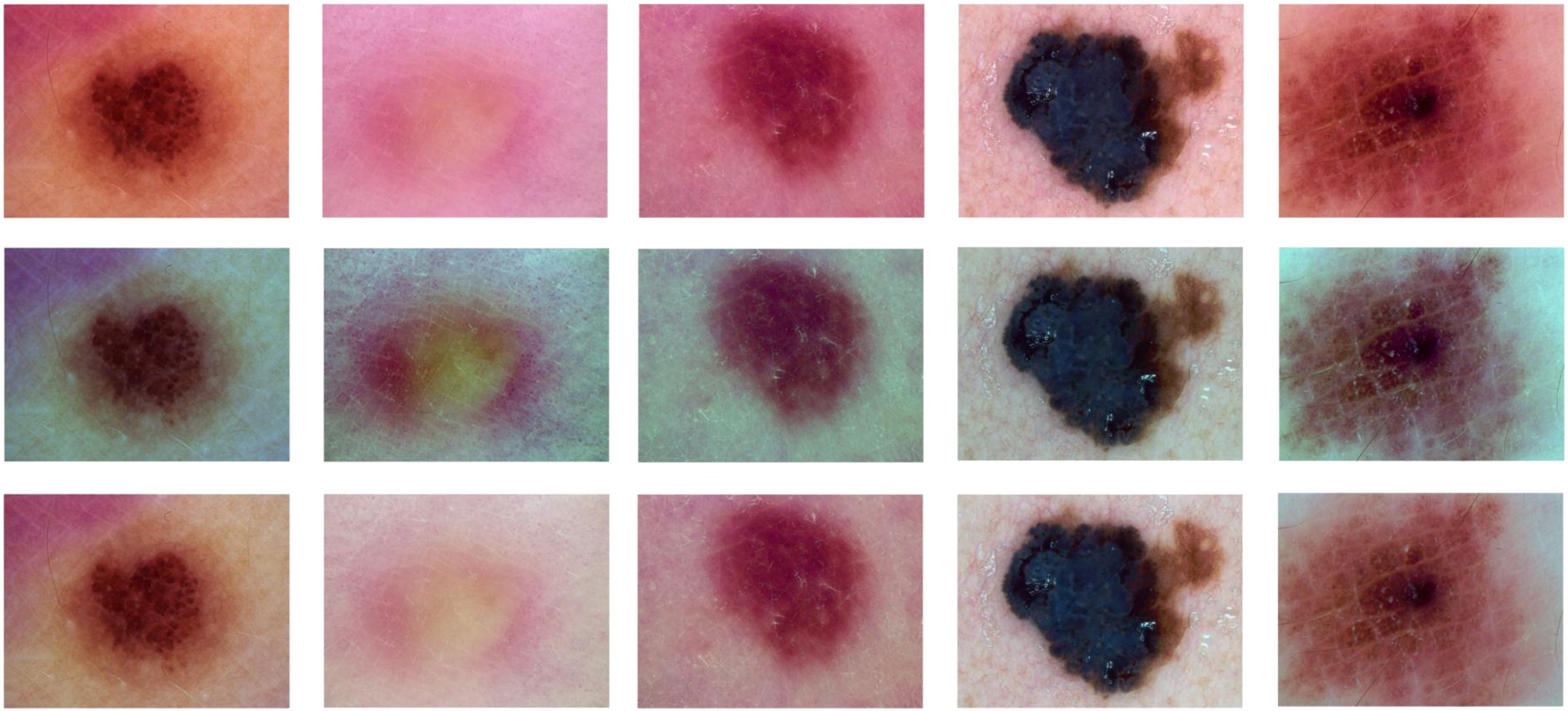

Figure 1: Original *RGB* images for 5 scans (top row) after applying ***Gray World Color Constancy*** (middle row) and ***MaxRGB Color Normalization*** (bottom row) transformations to achieve **color constancy**, i.e. detect color independent of the light source, and account for varying illumination and image acquisition conditions.

C. Barata et al. (2014), "Improving Dermoscopy Image Classification using Color Constancy", IEEE JBHI
G. Finlayson et al. (2004), "Shades of Gray and Color Constancy", 12th IS&T/SID Color Imaging Conf.
E. Land et al. (1971), "Lightness and Retinex Theory", Journal of Optical Society of America.

OCCLUSION REMOVAL & CLAHE

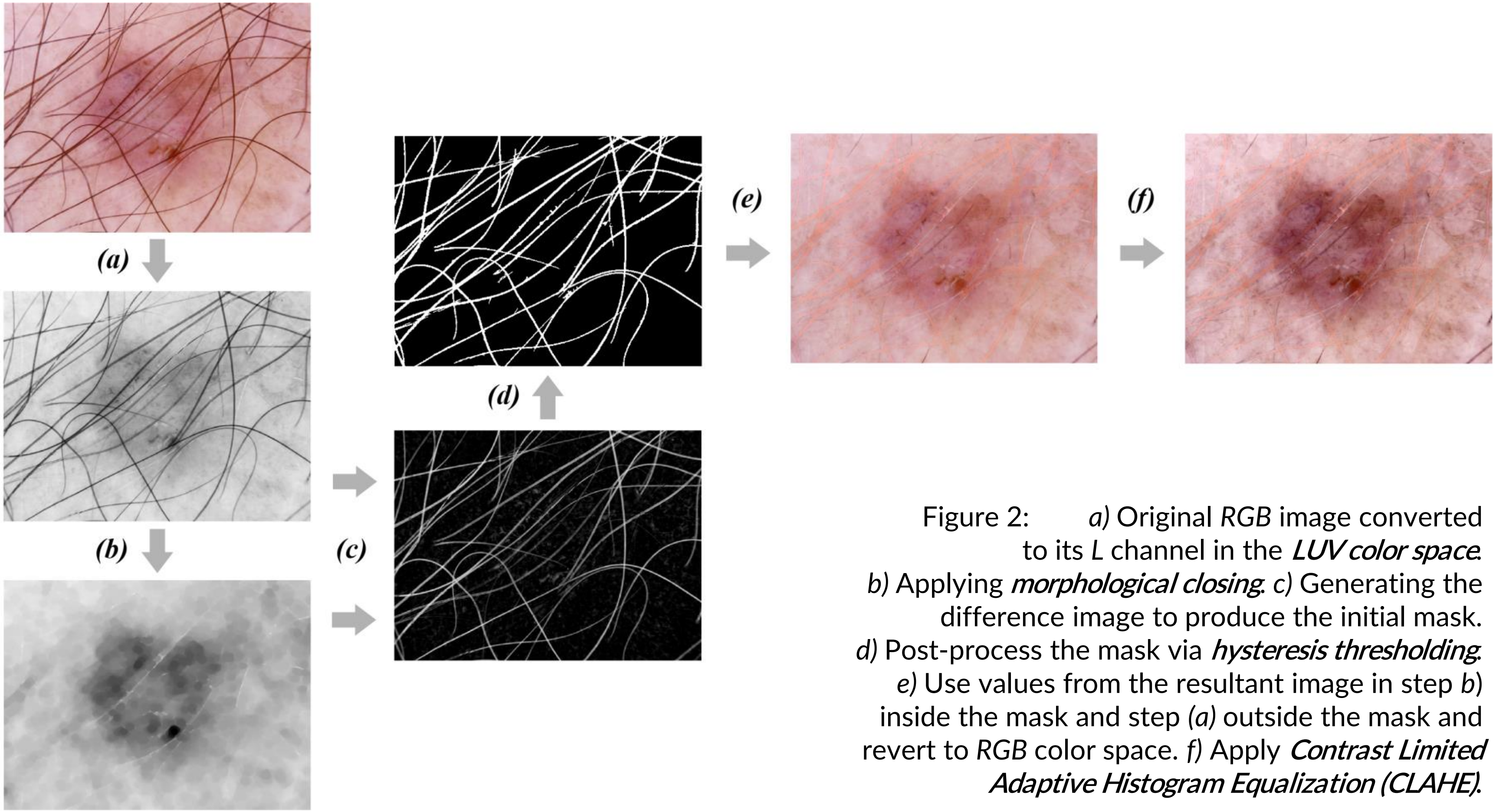

Figure 2: *a)* Original *RGB* image converted to its *L* channel in the ***LUV color space***. *b)* Applying ***morphological closing***. *c)* Generating the difference image to produce the initial mask. *d)* Post-process the mask via ***hysteresis thresholding***. *e)* Use values from the resultant image in step *b)* inside the mask and step *(a)* outside the mask and revert to *RGB* color space. *f)* Apply ***Contrast Limited Adaptive Histogram Equalization (CLAHE)***.

S. Saugeona et al. (2003), "Towards A Computer-Guided Diagnosis System for Pigmented Skin Lesions", Elsevier CMIG.
K. Zuiderveld (1994), "Contrast Limited Adaptive Histogram Equalization", Graphic Gems IV.

EM & K-MEANS SEGMENTATION

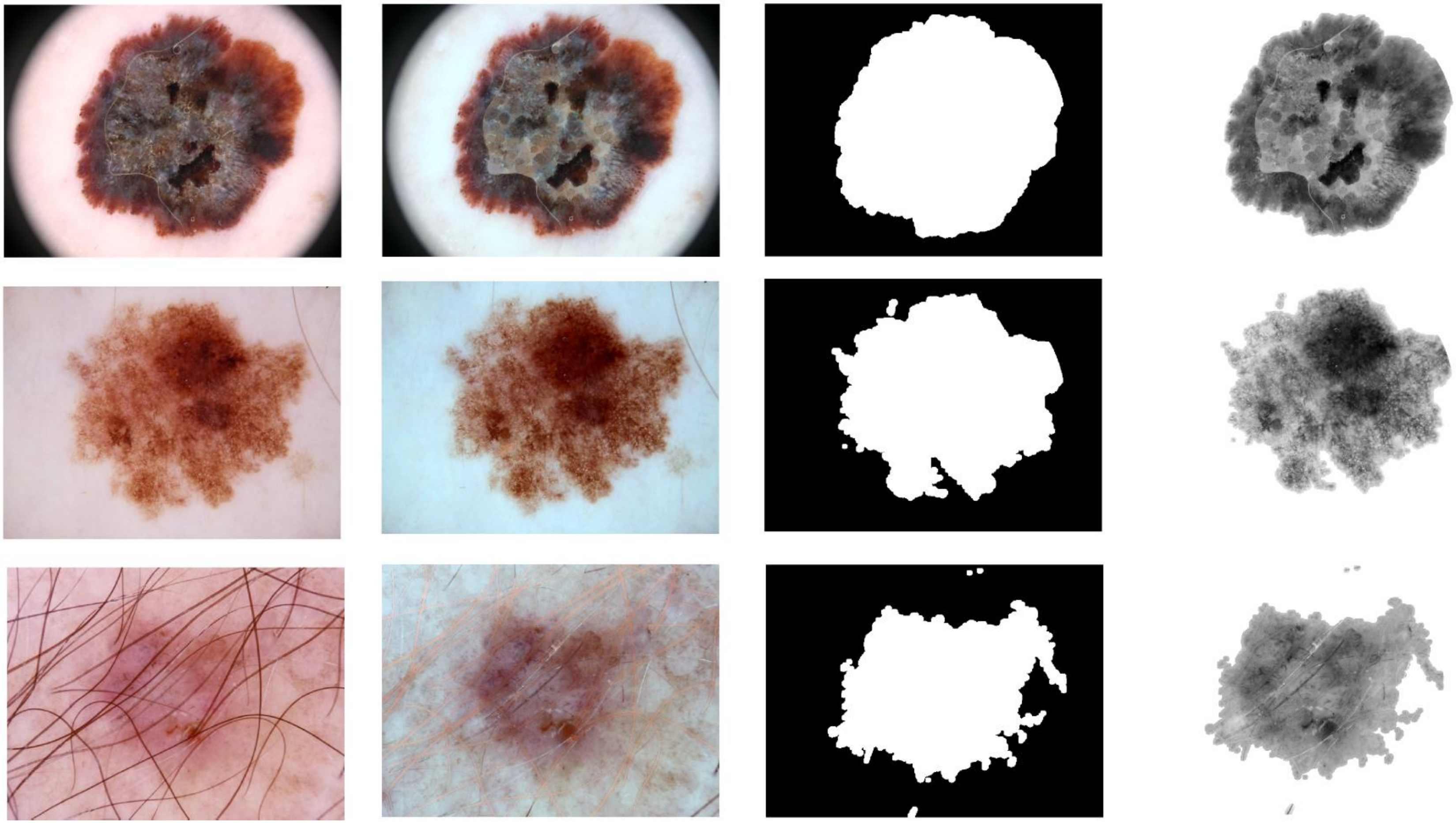

Figure 3: Original *RGB* images (left column) after preprocessing (second-from-left column), their segmented binary masks via ***K-Means*** clustering further refined using ***Expectation Maximization*** (second-from-right column) and the extracted skin lesion (right column).

H. Nisar et al. (2013) "A Color Space Study for Skin Lesion Segmentation", IEEE ICAS.

CHAN-VESE ACTIVE CONTOURS

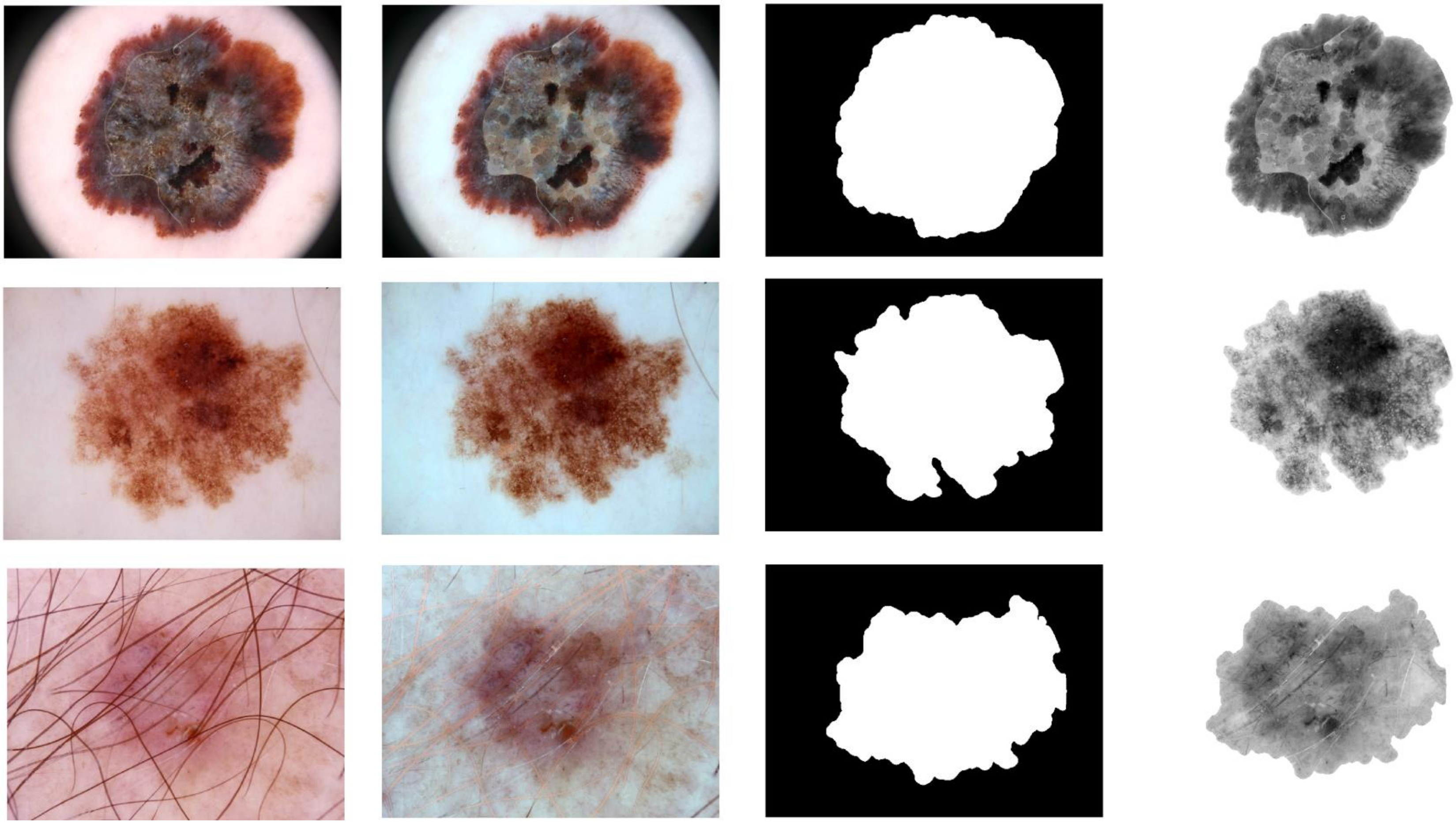

Figure 4: Original *RGB* images (left column) after preprocessing (second-from-left column), their segmented binary masks via ***Chan-Vese Active Contours*** algorithm over 5 iterations (second-from-right column) and the extracted skin lesion (right column).

T.F. Chan, L.A. Vese (2001), "Active Contours Without Edges", IEEE Transactions on Image Processing.

COLOR SPACES

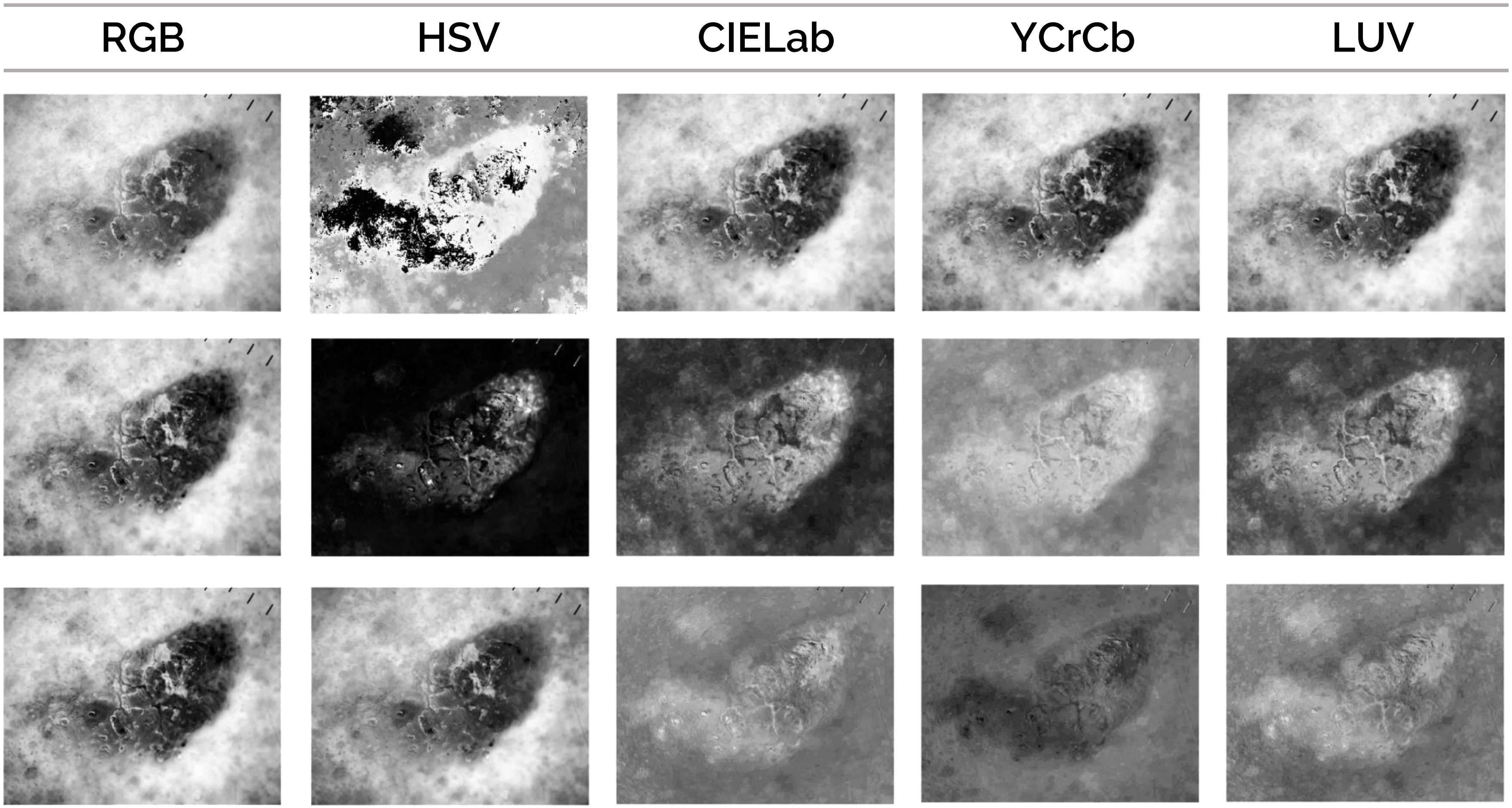

Figure 5: Color spaces used during computation of color moments and multi-color space texture features

A. Porebski et al. (2018), "Multi-Color Space LBP-Based Feature Selection for Texture Classification", SPIE JEI.
J. Yang et al. (2018), "Clinical Skin Lesion Diagnosis Using Representations Inspired by Dermatologist Criteria", IEEE CVPR.

MULTI-COLOR SPACE FEATURES

- **Color Moments**
  Mean, Standard Deviation, Skew, Kurtosis

- **Gray-Level Co-occurrence Matrix (GLCM)**
  Contrast, Dissimilarity, Homogeneity, Correlation, Entropy, ASM

- **Local Binary Patterns (LBP)**
  Points, P = 8; Radius, R = 2; Bins = 10

- **Melanoma Color Markers**
  Red, Black, White, Blue-Gray, Light Brown, Dark Brown

- **Basic Texture Features**
  Entropy, Smoothness, Uniformity

4 Features × 3 Channels × 5 Color Spaces × 2 Color Constancy Modes = **120 Features**

6 Features × 3 Channels × 5 Color Spaces × 2 Color Constancy Modes = **180 Features**

10 Features × 3 Channels × 5 Color Spaces × 2 Color Constancy Modes = **300 Features**

6 Features × 1 Color Space = **6 Features**

3 Features × 3 Channels × 5 Color Spaces × 2 Color Constancy Modes = **90 Features**

D. S. Gareau et al. (2016), "Digital Imaging Biomarkers Feed Machine Learning for Melanoma Screening," Exp. Derma.
A. Porebski et al. (2018), "Multi-Color Space LBP-Based Feature Selection for Texture Classification", SPIE JEI.
J. Yang et al. (2018), "Clinical Skin Lesion Diagnosis Using Representations Inspired by Dermatologist Criteria", IEEE CVPR.

GABOR WAVELETS

Gabor Wavelets
(0°, 22.5°, 45°, 67.5°, 90°, 112.5°, 135°, 157.5°, 180°)

Filter Response
(0°, 22.5°, 45°, 67.5°, 90°, 112.5°, 135°, 157.5°, 180°)

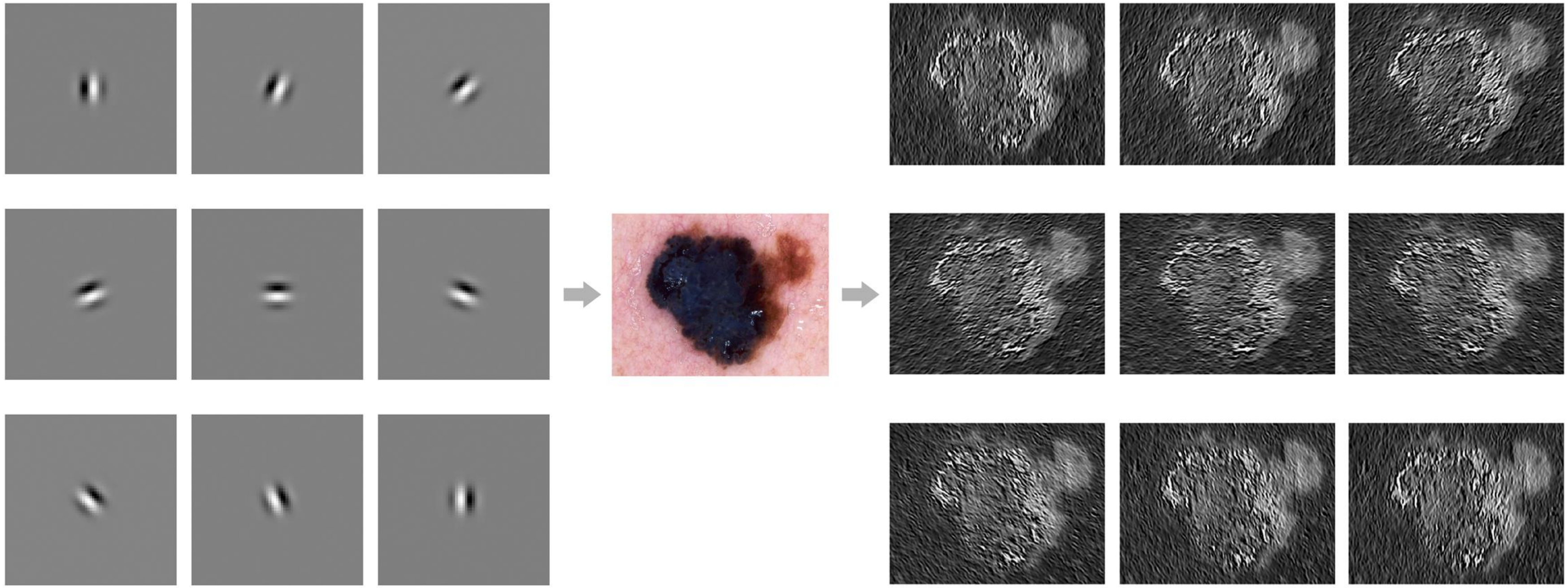

Figure 6: ***Gabor Filter*** response images and their respective local energy values for a *Gray-Level* image (converted from the original *RGB* image) constitute as 9 feature values to be used for texture classification.

M. Khaled et al. (2014), "A Hybrid System for Skin Lesion Detection: Based on Gabor Wavelet and Support Vector Machine", CISP

S. Serte et al. (2019), "Gabor Wavelet-Based Deep Learning for Skin Lesion Classification", Elsevier CBM.

HISTOGRAM OF GRADIENTS

Dermatoscopic Images

Histogram of Gradients (HOG) Features

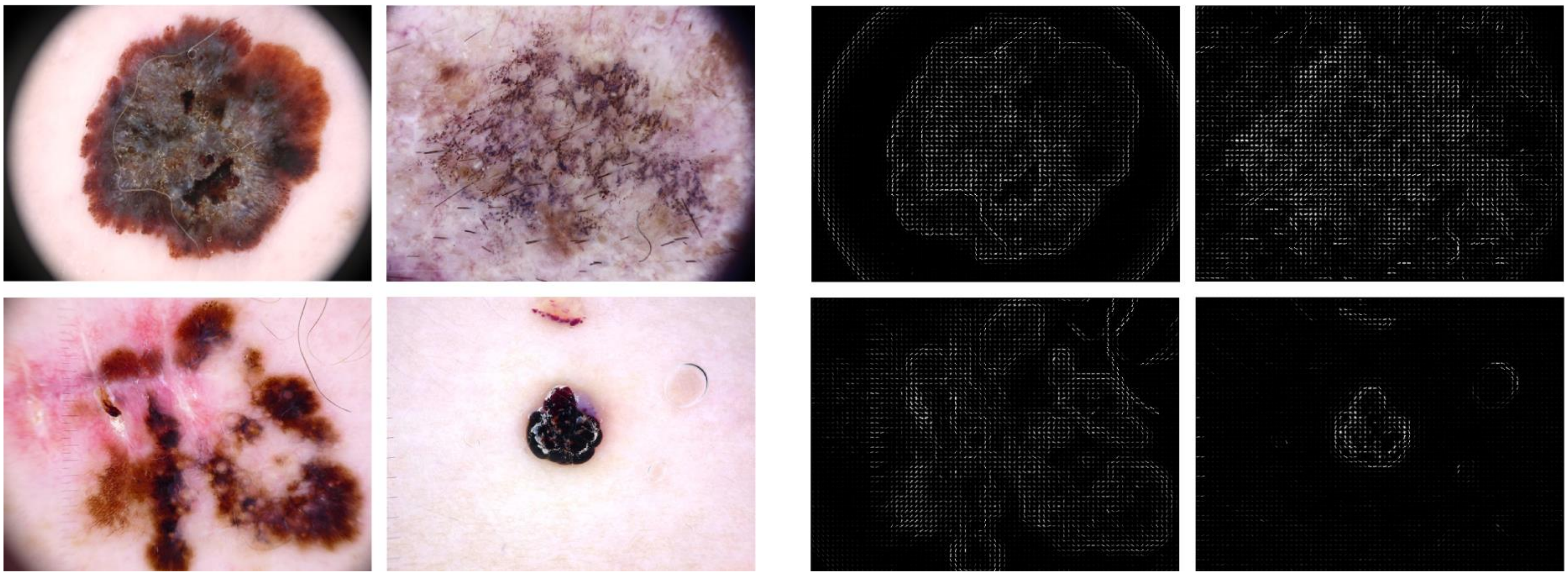

Figure 7: Multi-channel ***HOG Features*** (right) and their corresponding original *RGB* images (left) at 8 orientations, (8,8) pixels per cell and (1,1) cells per block.

S. Bakheet (2017), "An SVM Framework for Malignant Melanoma Detection Based on Optimized HOG Features", MDPI Comp.

H. Mahmoud et al. (2018), "Computer Aided Diagnosis System for Skin Lesions Detection using Texture Analysis Methods", ITCE

FEATURE SELECTION

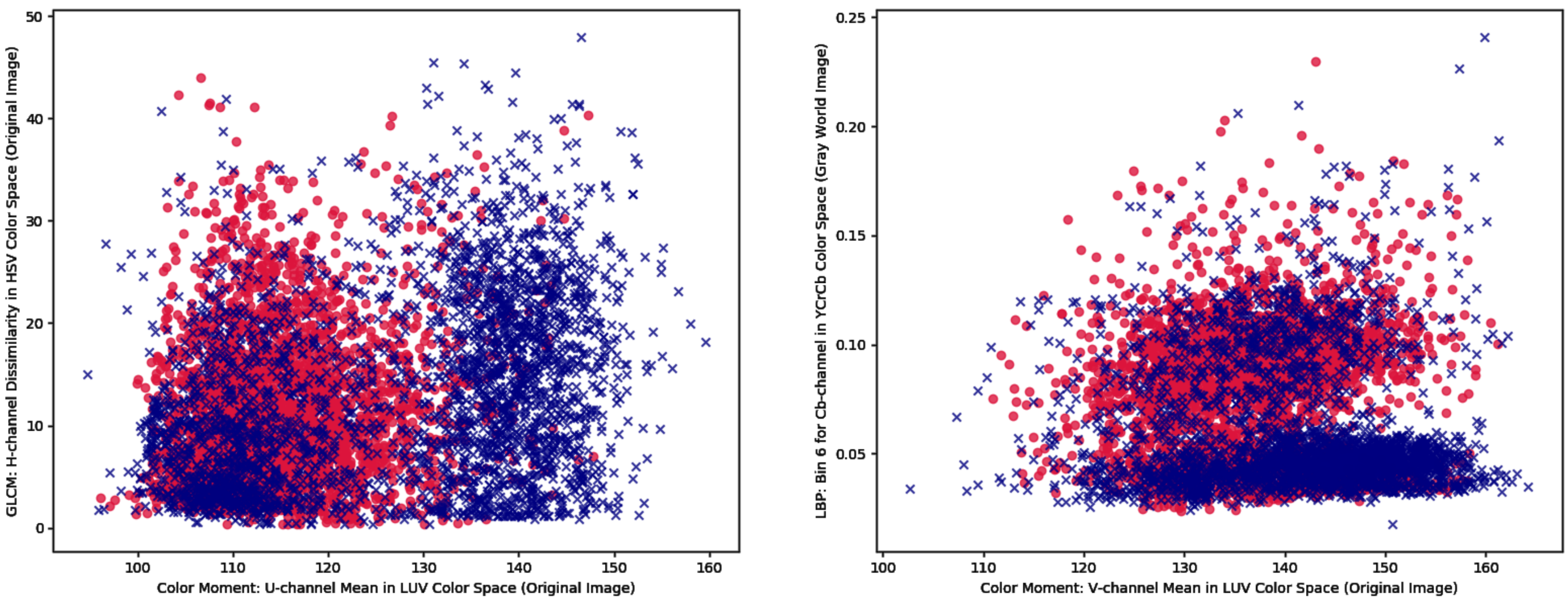

Figure 8: Scatter plot of all lesion samples (marked in red) and all nevus samples (marked in blue) in a 2-D feature space is used to assess the discriminative properties of any given pair of features. Highly redundant features are discarded in the final pipeline to streamline the training process and limit the potential risk of overfitting.

FINAL MODEL & OPTIMIZATION

PRE-PROCESS → **SEGMENT** → **EXTRACT FEATURES** → **CLASSIFY**

PRE-PROCESS

Gray World CC
~~White-Balance (LAB)~~
~~Gray-Edge CC~~
Max-RGB CC
~~Occlusion Removal~~
~~CLAHE~~

Lower Redundancy
Lower Data Distortion
Higher Accuracy
(≈+3%)

SEGMENT

~~EM, K-Means~~
~~C-V Active Contours~~
~~Watershed~~
Fixed Disc at Center

Faster Computation
Sensitivity over Specificity
Higher Accuracy
(≈+15%)

EXTRACT FEATURES

Color Moments
~~Shape Features~~
GLCM Features
LBP Features
Color Markers
Basic Texture Features
~~HOG Features~~
~~Gabor Wavelets~~
~~Relative Color Features~~

Lower Redundancy
Less Overfitting
Faster Computation
Higher Accuracy
(≈+30%)

CLASSIFY

SVM
~~Random Forests~~

Less Overfitting
Higher Accuracy
(≈+4%)

Y. Cheng et al. (2008), "Skin Lesion Classification using Relative Color Features", Skin Res Technol.

EXPERIMENTAL RESULTS

Metric	SVM	Random Forest
Accuracy	0.8992	0.8558
Precision	0.8992	0.8584
Recall	0.8992	0.8558
F1 Score	0.8992	0.8556
Sensitivity	0.9030	0.8980
Specificity	0.8950	0.8130
AUC	0.9578	0.9419

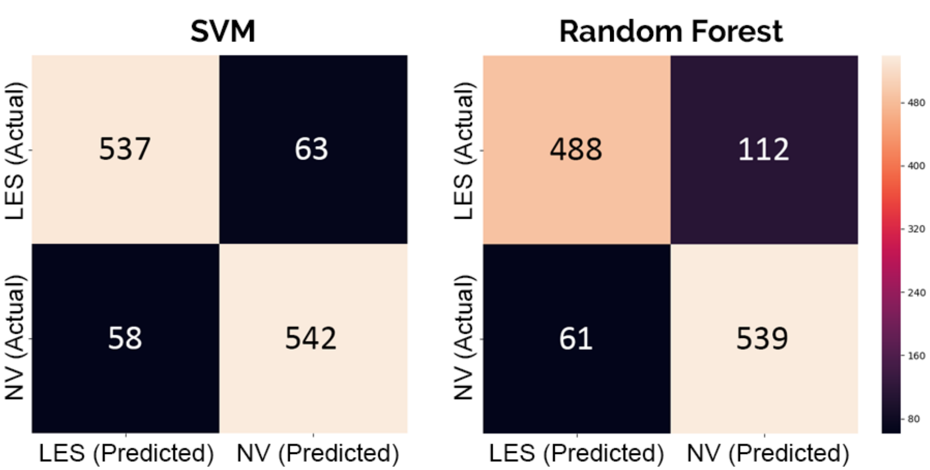

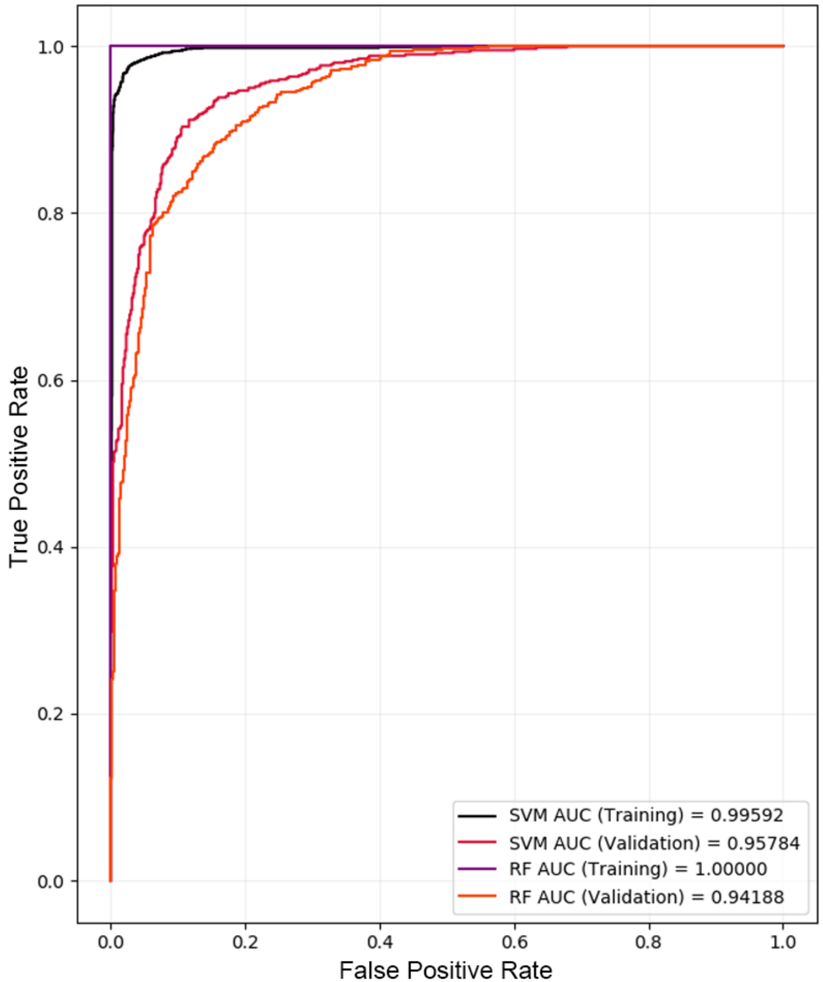

Figure 9: Evaluation metrics, confusion matrices and Receiver Operating Characteristic (ROC) curve for SVM and Random Forest on the validation set, after performing grid search to tune each classifier.

FUTURE WORK

Challenges

- Performing **computationally efficient unsupervised segmentation** with high sensitivity and specificity, while preserving accurate contour information.

- Improved **occlusion (black/white hair, markers) removal** while preserving details from smaller, darker lesions and ensuring **minimal data distortion**.

- Determining the **most reliable localized shape/texture features to discriminate nevi** from all other classes of skin lesions sharing a wide range of shape properties.

- Advanced **classification strategies to optimize computation time and accuracy** (e.g. cascaded SVM with weak features in the starting layer, and increasingly more discriminating features through the subsequent layers, ensuring that every feature is not calculated for every sample).